Reports

ROSAT Detection of an X-ray Shadow in the 1/4-keV Diffuse Background in the Draco Nebula

S. L. SNOWDEN, U. MEBOLD, W. HIRTH, U. HERBSTMEIER, J. H. M. M. SCHMITT

The detection by the Roentgen satellite (ROSAT) x-ray telescope of a shadow in the 1/4–kiloelectron volt (C band, 0.1 to 0.284 kiloelectron volt) cosmic diffuse background is reported. The location and morphology of the local minimum in x-rays are in clear agreement with a discrete H I cloud. The shadow is very deep with a minimum level at 50 percent of the surrounding emission; therefore, a minimum of 50 percent of the observed off-cloud flux must originate on the far side of the cloud. The analysis of H I velocity components links the cloud with the Draco nebula (distance ~600 parsecs); it then follows that there is significant 1/4–kiloelectron volt x-ray emission at a large distance (>400 parsecs) from the galactic plane along this line of sight. The extent of the distant emission region is uncertain, and, if it indicates the existence of a hot galactic corona, it must be patchy in nature.

THE 1/4-KEV COSMIC SOFT X-RAY diffuse background (SXRB) was first detected over two decades ago (*1, 2*), yet the spatial distribution of the source or sources responsible for this emission is still uncertain. It was quickly noted that there is a negative correlation between the SXRB and galactic neutral hydrogen as measured by 21-cm line emission. The negative correlation led to the absorption model, which postulated that the spatial variation of the x-ray intensity is due to the absorption of a galactic halo by the foreground interstellar medium (ISM) (*1*). During the next decade the absorption model was refined and modified to include such features as a local emission component to account for the finite flux in the galactic plane and a clumped ISM to account for fitted absorption cross sections, which are much smaller than the theoretical values (*3*). During the 1980s the pure two-component absorption model fell into disfavor as its failures became more apparent (*4*).

There are currently two alternative models for the SXRB; both assume that the bulk of the emission is galactic in origin. One [the displacement model (*5*) and references therein] states that most of the observed flux arises from a hot (10^6 K) plasma contained in a local cavity of limited (less than a few hundred parsecs) extent surrounding the sun and that the spatial variation is due in large part to variations in the extent of the cavity (and therefore plasma emission measure). The other [the interspersed model (*6, 7*)] states that the hot plasma is distributed extensively in the galaxy intermixed with the cooler x-ray–absorbing ISM and that a significant fraction of the observed flux originates as coronal emission. The spatial variation is due to global structure in the distribution of x-ray emission regions and cooler absorbing H I. There is broad agreement that the sun lies in a region of x-ray–emitting plasma. The difference between the models depends on whether the observed variation in intensity is due primarily to local geometry or to global structure.

The most direct way to determine the distribution of emission responsible for the observed 1/4-keV flux is to search for shadowing by absorbing features at known distances. This has been attempted for a few targets [Small Magellanic Cloud and the intervening galactic H I (*8, 9*); galactic H I features (*10*)], and no significant absorption has been detected. However, the instruments available in the past were not optimal for such a search. Either the exposure or the position resolution, or both, were insufficient to observe small-scale features [for example, the Wisconsin survey (*4*)] or background levels were too high and 1/4-keV sensitivities were too low (for example, the Einstein imaging proportional counter).

The situation has now changed with the launch and operation of ROSAT (*11*). The fast optics of the x-ray telescope [XRT (*12*)] combined with the high quantum efficiency and low background of the position-sensitive proportional counter [PSPC (*13*)] provide an ideal instrument for the study of the SXRB. It will be possible with ROSAT to map out in detail the local distribution of x-ray–emitting material. With the completion of the all-sky survey, we are now searching for absorption features over nearly the entire sky. We report here the detection of the first such shadow. Fortuitously, the shadow is in the region of the Draco nebula where the galactic H I has been extensively studied at high resolution (9 arc min) with the Effelsberg 100-m radio telescope (*14*), and a distinct cloud responsible for the shadow is clearly identifiable.

The x-ray data were collected by the ROSAT XRT/PSPC during the survey verification phase of operations between 12 and 15 July 1990. During survey operations, ROSAT scans in such a way that one great circle is swept out on the sky each orbit. The plane of the great circle is rotated by 4 arc min each orbit around the line connecting the ecliptic poles. With this geometry, the region of interest was observed for 30 s each orbit for roughly 50 orbits (3.5 days). Because some exposure is occasionally lost as a result of dead time in the particle belts, the total exposure, though not constant over the cloud, was roughly 1100 s.

Figure 1 shows the background-subtracted C band x-ray image of the region. The field is 1.8° in diameter, and the center is located at galactic longitude ℓ ~94.7°, latitude b ~ 37.6° with longitude increasing to the left and the north galactic pole up. The intensity varies strongly over the field with a

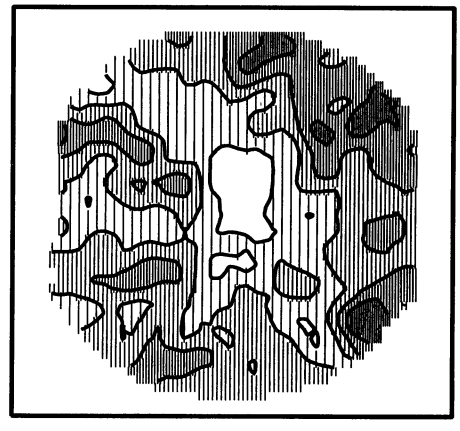

Fig. 1. Smoothed x-ray image of the shadow. The minimum contour is at 6×10^{-4} count s^{-1} arc min^{-2} with contour intervals of 2×10^{-4} count s^{-1} arc min^{-2}. The field is 1.8° in diameter with the center at ℓ ~94.7°, b ~37.6°; longitude increases to the left and the north galactic pole is up.

S. L. Snowden, Max-Planck-Institut für Extraterrestrische Physik, D-8046 Garching bei München, Federal Republic of Germany, and Department of Physics, University of Wisconsin, Madison, WI 53706.
U. Mebold, W. Hirth, U. Herbstmeier, Radioastronomisches Institut der Universität Bonn, Bonn, Federal Republic of Germany.
J. H. M. M. Schmitt, Max-Planck-Institut für Extraterrestrische Physik, D-8046 Garching bei München, Federal Republic of Germany.

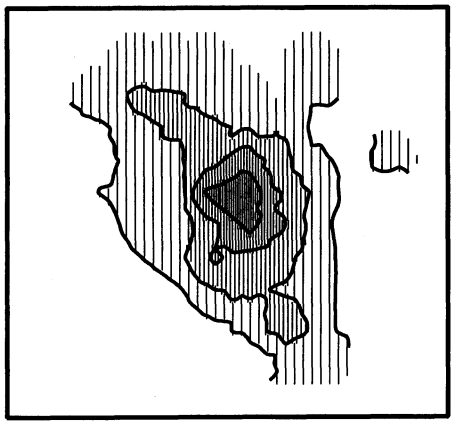

Fig. 2. Smoothed galactic $N_{H\,I}$ image of the cloud (velocity interval: -30 km s^{-1} < $V_{H\,I}$ < -17 km s^{-1}). The field is the same as for Fig. 1; the minimum contour is 0.5×10^{20} H I cm^{-2} with contour intervals of 0.5×10^{20} H I cm^{-2}.

deep local minimum at the center. It is this local minimum with a count rate of roughly 50% of the surrounding region that is the shadow. These data [and the following H I and Infrared Astronomical Satellite (IRAS) data] have been smoothed over a radius of 7.5 arc min only for the purpose of display.

The noncosmic background of the observation can be separated into two components. The first component is induced in the PSPC by high-energy particles and is both well understood (*15*) and small (roughly 1% of the cosmic background). The second component is of greater magnitude and of uncertain origin. The XRT/PSPC occasionally experiences soft (C band) and relatively isotropic (less than a factor of 2 variation in intensity during an orbit) noncosmic background enhancements that are independent of zenith angle, satellite day-night status, and geomagnetic latitude and typically last

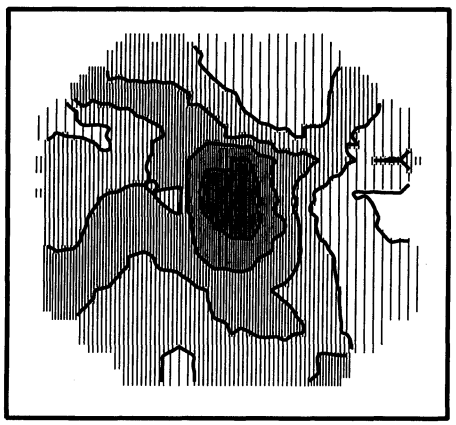

Fig. 3. Smoothed galactic $N_{H\,I}$ image of the cloud region (velocity interval: -80 km s^{-1} < $V_{H\,I}$ < 20 km s^{-1}). The field is the same as for Fig. 1; the minimum contour is 2.0×10^{20} H I cm^{-2} with contour intervals of 0.5×10^{20} H I cm^{-2}.

slightly less than a day. During this observation, the satellite experienced such an enhancement, which we estimate contributed an average $\sim 0.9 \times 10^{-4}$ count s^{-1} arc min^{-2} and is roughly 10% of the cosmic background in the target direction. There is no apparent structure to the distribution of these excess counts across the field of view, although study of both their spatial and spectral distribution in the detector as well as their temporal evolution continues. Because the x-ray image is the sum of many scans at various off-axis angles, any possible nonuniformity in the distribution of excess counts will be smoothed. The counts were modeled as a constant contribution to the observed flux, and in no way could this component or the subtraction of it produce the observed shadow. (Multiple coverage of the region during the 3.5-day period allowed the identification of the enhancement and an accurate determination of its magnitude.) The target direction was observed during satellite night, and the observation is uncontaminated by scattered solar x-rays.

The H I data were measured in 1983 with the 100-m radio telescope in Effelsberg as an extension of a previously studied field (*16*). The spectra were sampled on a regular grid of 10′ by 10′ in galactic longitude and latitude (spacing along ℓ was in true angles). The beam width was 9′, the spectral resolution was 1.69 km s^{-1}, and the data were corrected for stray radiation by the method of Kalberla *et al.* (*17*).

To separate the cloud H I from the rest of the gas, the spectra have been decomposed into Gaussian components. Figure 2 shows the column density map for the Gaussian components representing the Draco nebula (velocity width <11.8 km s^{-1} and radial velocity -30 km s^{-1} < v < -17 km s^{-1}). Figure 3 shows the column density map for all atomic hydrogen in the velocity range -80 km s^{-1} < v < 20 km s^{-1}.

CO line emission is found at the densest parts of the clump within a radius of 8′ around the central position (*18*), implying the presence of significant quantities of molecular hydrogen. To account for this additional column density of hydrogen nuclei, we also compare the x-ray shadow with the 100-μm intensity, I_{100}, measured by IRAS, which is proportional to the total hydrogen column density (*19*). An IRAS 100-μm map in the area of the x-ray shadow is shown in Fig. 4. To compare the x-ray shadow with the infrared emission, we have subtracted the contribution of zodiacal light and a galactic background of 6.2 MJy sr^{-1} and then converted the residual I_{100} intensity into the total hydrogen column density of the cloud, N_{H_2}, by the conversion factor 1×10^{20} H cm^{-2} MJy^{-1} sr derived for the

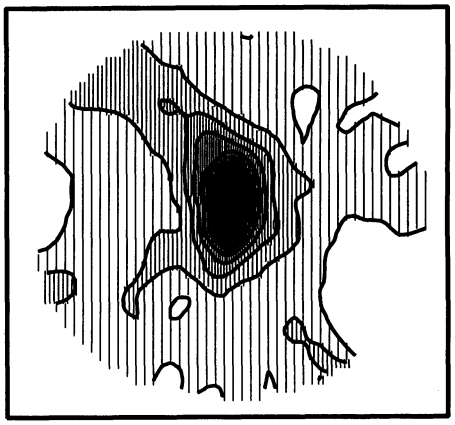

Fig. 4. Smoothed IRAS 100-μm image of the cloud. The field is the same as for Fig. 1; the minimum contour is 0.5 MJy sr^{-1} with contour intervals of 0.5 MJy sr^{-1}.

Draco nebula (*20*).

The distance of the Draco nebula has been derived by various researchers and different methods. Most recently, a distance range of 300 to 1500 pc with a most probable distance of roughly 600 pc has been derived (*14*). The H I cloud seen as an x-ray shadow

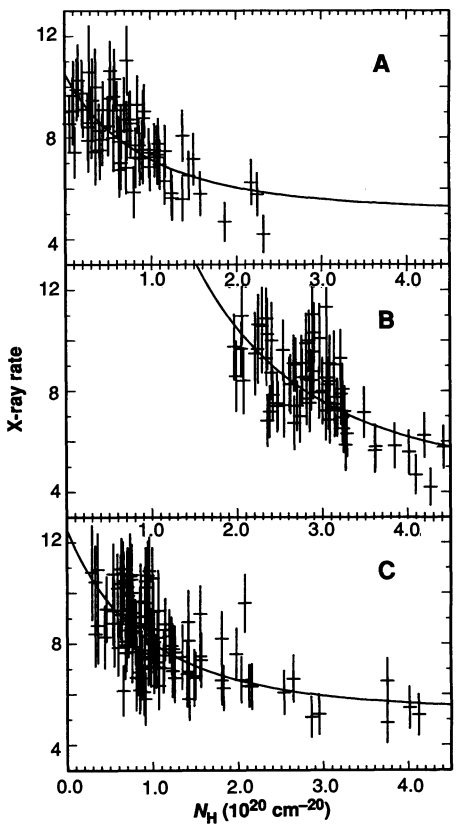

Fig. 5. (**A**) X-ray versus cloud H I scatter plot. X-ray count rate in units of 10^{-4} count s^{-1} arc min^{-2}. Curve shows the best-fit model. (**B**) Same as (A) except x-ray versus total galactic H I. (**C**) Same as (A) except x-ray versus total cloud hydrogen column density N_H derived from I_{100}.

is very likely a part of the Draco nebula because (i) the radial velocity, $v \sim -24$ km s^{-1}, is typical for the rest of the Draco nebula (*16*) and (ii) the dust and molecular content of the cloud are similar to the rest of the Draco nebula and deviate significantly from those of molecular clouds typical of the galactic disk (*20*).

In order to determine the foreground and background fractions of the observed x-ray flux relative to the cloud, we considered the on-cloud and off-cloud data as an ensemble. We binned the x-ray data so as to provide matched values with the hydrogen observations. In practice, this meant binning the x-ray data in a region 10 arc min in diameter centered on the pointing direction of each 21-cm spectrum. This was repeated for the two 21-cm velocity intervals (all galactic H I and those velocities associated with the Draco nebula) and for the IRAS 100-μm data after changing the grid to 9 arc min.

The data were then fitted by a two-component absorption model:

$$I_x = I_0 + I_1 e^{-\sigma(N_H)N_H}$$

where I_x is the observed x-ray intensity; I_0 and I_1 are, respectively, the foreground and background (relative to the cloud or total H I) intensities; σ is the band-averaged x-ray absorption cross section per hydrogen atom; and N_H is the hydrogen column density. The cross section, σ, is fixed to the theoretical value determined by folding a Raymond (*21*) 10^6 K thermal emission model through the ISM x-ray absorption model of Morrison and McCammon (*22*) and the XRT/PSPC response function. The cross section is not constant but decreases with increasing hydrogen column density as a result of the hardening of the residual spectrum. In the fits, I_0 and I_1 are allowed to vary. Table 1 shows the results of the fits, the χ^2_ν values, and the degrees of freedom ν. The uncertainties quoted are the 1σ errors based on the use of the Lampton, Margon, and Bowyer (*23*) criteria; in this case, the 1σ level corresponds to an increase of 2.3 in the χ^2 value. Both the fit based on the intermediate velocity H I and the fit based on the IRAS 100-μm data are formally acceptable (fits 1 and 3); the fit based on the total galactic H I column density is marginal (fit 2). However, they exhibit a consistent value for the foreground component and strongly significant nonzero values for the background component with similar values for the relative uncertainties. Figure 5, A, B, and C, shows the scatter plots with the best-fit models. These results support the attribution of the SXRB local minimum to shadowing by the cloud. Not only is there clear positional and morphological agreement between the cloud location and the x-ray intensity minimum, but also the modulation of x-ray intensity by cloud absorption is consistent with theoretical predictions.

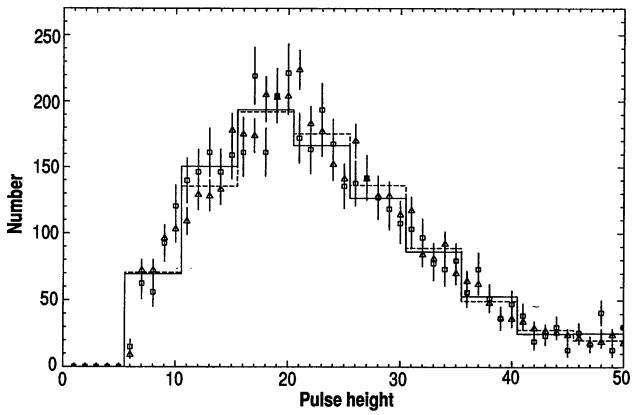

Fig. 6. On-cloud (squares and binned solid curve) and off-cloud (triangles and binned dashed curve) pulse-height spectra. The on-cloud data have been scaled for comparison. One channel is roughly 10 eV.

The on-cloud and off-cloud pulse-height spectra for the 1/4-keV energy band are shown in Fig. 6 (the on-cloud data have been scaled for comparison). There is little readily apparent difference in spectral shape between the two, which implies that the foreground and background spectra as observed by ROSAT are similar. This result is somewhat surprising as partial absorption will harden a spectrum (if there is any trend in the data, it is toward a softer on-cloud spectrum). Unfortunately, we do not have sufficient counts at this time to study in detail the variation of spectra with cloud column density (where some variation in spectral shape would be expected). This will be studied in great detail when all of the ROSAT survey data for the entire Draco region are available.

The important result of this paper is the observation of a deep shadow (~50%) in the 1/4-keV diffuse background associated with a discrete cloud in the interstellar medium. The identification of the depression in the count rates of Fig. 1 as the x-ray shadow of the gas and dust cloud in Figs. 2, 3, and 4 is based on the coincidence of their position, their morphology, and the consistency of the theoretical absorption cross section with the data as shown in Fig. 5. The cloud appears to be associated with the Draco nebula, which has been located at a probable distance of 600 pc.

Our model fits to the x-ray count rate and hydrogen column density distributions allow conclusions about the emission measures of the foreground region (the local bubble) and background (emission in the halo with distance >400 pc). With the simplifying assumption that the observed flux, I_0, originates not only in front of the specific cloud but also on the near side of the low-velocity gas, a local emission measure of $n_e^2 d \sim 1.8 \times 10^{-3}$ cm^{-6} pc [temperature $\sim 10^6$ K (*5*)] is implied. Parameters of the local x-ray emission region (*5*) indicate an electron density, n_e, between 3.7×10^{-3} and 4.7×10^{-3} cm^{-3}. This implies a path length in the local emission region of 80 to 130 pc, which is consistent with the distance to the low-velocity H I (*14*). The flux of distant origin, I_1, when corrected for absorption by the low-velocity gas (see Figs. 3 and 5B and fit 2), implies an emission measure of $\sim 1.3 \times 10^{-2}$ cm^{-6} pc, an order of magnitude higher than the local emission measure. A similar emission measure is derived from the model fit to the column densities inferred from the IRAS data (fit 3) if the x-ray count rates are corrected for foreground absorption (see above).

The conclusion that at least 50% of the observed 1/4-keV flux in the direction of the Draco nebula originates on the far side of the nebula follows from the first unambiguous discovery of a C band x-ray shadow cast by a discrete H I feature. However, we believe that the existence of this shadow does not imply the existence of an extensive and homogeneous galactic halo or significant extragalactic emission for three specific reasons. First, preliminary results from the ROSAT sky survey indicate that in the

Table 1. Fitted parameters. I_0 and I_1 have the units 10^{-4} count s^{-1} arc min^{-2}.

Fit	Hydrogen	Foreground (I_0)	Background (I_1)	χ^2_ν	ν
1	Draco nebula	5.1 ± 0.5	5.4 ± 1.0	1.061	63
2	Total	4.5 ± 0.6	34.2 ± 5.6	1.205	72
3	IRAS 100 μm	5.3 ± 0.4	7.2 ± 1.0	1.076	119

direction of the minimum column density of galactic H I [$\sim 5 \times 10^{19}$ H I cm^{-2}, $\ell \sim 151.6°$, $b \sim 52.1°$ (*24*)], there is not a correspondingly high x-ray intensity. An emission measure of $\sim 1.3 \times 10^{-2}$ cm^{-6} pc would generate a count rate roughly three times what is observed in that direction. Because the two directions are not far from each other on the sky (~35°), this is difficult to reconcile in the case of an extensive x-ray halo. Second, the Draco nebula lies in the direction of a large complex of high-velocity clouds (HVCs) and it is possible that the background x-ray emission could be a relatively isolated phenomenon indicative of an interaction between the HVCs and the cooler gas in the galactic halo. Third, although the H I velocity information of the shadowing cloud strongly links the cloud to the Draco nebula, it will still be reassuring to have the distance confirmed by ISM absorption line measurements or the detection of shadowing by the rest of the Draco nebula.

This result illustrates the utility of ROSAT XRT/PSPC observations in a search for SXRB shadowing. Any discrete absorbing feature with a known distance is a target for such a search, and the observed flux can be divided into foreground and background emission. With a sufficient number of targets, we can bypass both the displacement model and interspersed model with their limitations of treating only the general appearance of the SXRB and map out in detail the distribution of x-ray emission in the solar neighborhood. This same analysis can be extended to the higher energy M band (0.5 to 1.0 keV) and greater sample distances from the sun (~1 kpc in the galactic plane). One caveat, however, is that, although ROSAT survey data are in general usable in the search for C band shadows if an accuracy of 5 to 10% in the fraction determination is sufficient, a search for M band shadows will require the greater exposure of a pointed observation.

REFERENCES AND NOTES

1. C. S. Bowyer, G. B. Field, J. E. Mack, *Nature* **217**, 32 (1968).
2. A. N. Bunner, *et al.*, *ibid.* **223**, 1222 (1969).
3. F. J. Marshall and G. W. Clark, *Astrophys. J.* **287**, 633 (1984).
4. D. McCammon, D. N. Burrows, W. T. Sanders, W. L. Kraushaar, *ibid.* **269**, 107 (1983).
5. S. L. Snowden, D. P. Cox, D. McCammon, W. T. Sanders, *ibid.* **354**, 211 (1990).
6. P. Jakobsen and S. M. Kahn, *ibid.* **309**, 682 (1986).
7. W. Hirth, U. Mebold, M. Dahlem, P. Müller, *Astrophys. Space Sci.*, in press.
8. D. McCammon, A. N. Bunner, P. L. Coleman, W. L. Kraushaar, *Astrophys. J.* **168**, L33 (1971).
9. D. McCammon, S. S. Meyer, W. T. Sanders, F. O. Williamson, *ibid.* **209**, 46 (1976).
10. D. N. Burrows, D. McCammon, W. T. Sanders, W. L. Kraushaar, *ibid.* **287**, 208 (1984).
11. J. Trümper, *Adv. Space Res.* **2**, 241 (1983).
12. B. Aschenbach, *Appl. Opt.* **27** (no. 8), 1404 (1988).
13. E. Pfeffermann *et al. Proc. SPIE Int. Soc. Opt. Eng.* **733**, 519 (1987).
14. D. Lilienthal, A. Wennmacher, U. Herbstmeier, U. Mebold, *Astron. Astrophys.*, in press.
15. S. L. Snowden and P. P. Plucinsky, in preparation.
16. W. Goerigk, U. Mebold, K. Reif, P. M. W. Kalberla, L. Velden, *Astron. Astrophys.* **120**, 63 (1983).
17. P. M. W. Kalberla, U. Mebold, W. Reich, *ibid.* **82**, 275 (1980).
18. U. Herbstmeier, R. Rohlfs, U. Mebold, in *The Physics and Chemistry of Interstellar Molecular Clouds*, G. Winnewisser and J. T. Armstrong, Eds. (Lecture Notes in Physics No. 331, Springer-Verlag, Berlin, 1989), p. 195.
19. A. Heithausen and U. Mebold *Astron. Astrophys.* **214**, 347 (1989).
20. U. Herbstmeier, thesis, Universität Bonn (1990).
21. J. C. Raymond, in *Hot Thin Plasmas in Astrophysics*, R. Pallavicini, Ed. (Kluwer Academic, Dordrecht, 1988), p. 3.
22. R. Morrison and D. McCammon, *Astrophys. J.* **270**, 119 (1983).
23. M. Lampton, B. Margon, S. Bowyer, *ibid.* **208**, 177 (1976).
24. K. Jahoda, F. J. Lockman, D. McCammon *ibid.* **354**, 184 (1990).

25. We thank B. Wakker for providing the IRAS 100-μm map corrected for scanning effects. We also acknowledge useful discussions with K. Jahoda, D. McCammon, and W. Sanders. This work was supported in part by the Max Planck Institute for Extraterrestrial Physics, the National Aeronautics and Space Administration under grants NAG 5-1438 and NAG 5-629, and the Deutsche Forschungsgemeinschaft under grant ME 745/7-2.

11 April 1991; accepted 2 May 1991

Crystallinity of the Double Layer of Cadmium Arachidate Films at the Water Surface

F. LEVEILLER, D. JACQUEMAIN, M. LAHAV, L. LEISEROWITZ, M. DEUTSCH, K. KJAER, J. ALS-NIELSEN

A crystalline counterionic layer at the interface between an electrolyte solution and a charged layer of insoluble amphiphilic molecules was observed with grazing incidence synchrotron x-ray diffraction. Uncompressed arachidic films spread over 10^{-3} molar cadmium chloride solution (pH 8.8) spontaneously form crystalline clusters with coherence lengths of ~1000 angstroms at 9°C. Ten distinct diffraction peaks were observed, seven of which were attributed to scattering only from a crystalline Cd^{2+} layer and the other three to scattering primarily from the arachidate layer. The reflections from the Cd^{2+} layer were indexed according to a 2 × 3 supercell of the arachidate lattice with three Cd^{2+} ions per cadmium unit cell.

THE INTERFACIAL REGION BETWEEN a charged surface and an electrolyte is central to many processes such as those occurring during electrodeposition, ion transport through biological membranes, preparation of Langmuir-Blodgett films (*1*), biomineralization (*2*), and induced oriented nucleation of inorganic systems (*3*) under Langmuir monolayers. The use of direct methods such as grazing incidence x-ray diffraction (GID) and specular x-ray reflection (XR), when applied to films spread on the surface of liquids, has demonstrated that the surfactant molecules can acquire in-plane long-range order (*4–6*) and that metal ions, when present in solution, interact closely with the charged monolayer head groups at the interface (*7*). However, it was not known whether the ion distribution near such charged, ordered surfaces may be crystalline, particularly if the monolayer is singly charged and the counterion doubly charged (*8, 9*). In such a system, a monolayer not fully ionized may induce short-range order of the counterionic layer with the possibility of an incommensurate structure to meet charge neutrality. On the other hand, if the monolayer is fully ionized, the counterionic layer may still be incommensurate with that of the monolayer or may be arranged in a supercell.

X-ray standing waves were recently used to demonstrate that the Zn^{2+} double layer at a phospholipid membrane–aqueous interface is diffuse (*10*). Liquid-surface extended x-ray absorption fine structure (EXAFS) spectroscopy experiments on manganese stearate films (*11*) at room temperature yielded a Mn–Mn nearest neighbor distance at the surface in the compressed phase only, indicating at least short-range order. GID measurements of lead arachidate (*5*) monolayers at room temperature gave no indication of ordering of the Pb^{2+} ions. Here we describe a GID study of uncompressed cadmium arachidate monolayers at 9°C, which demonstrates the presence of an ordered Cd counterionic layer of a unit cell commensurate with, but larger than, that of the arachidate monolayer.

For these measurements we used the liquid-surface diffractometers on the wiggler

F. Leveiller, D. Jacquemain, M. Lahav, L. Leiserowitz, Structural Chemistry Department, Weizmann Institute of Science, Rehovot 76100, Israel.
M. Deutsch, Physics Department, Bar-Ilan University, Ramat-Gan 52100, Israel.
K. Kjaer and J. Als-Nielsen, Physics Department, Risø National Laboratory, DK4000 Roskilde, Denmark.